Journal of Sound and Vibration (2000) **230**(1), 149–170
doi:10.1006/jsvi.1999.2610, available online at http://www.idealibrary.com on IDEAL®

SOUND INSULATION OF DOORS—PART 2: COMPARISON BETWEEN MEASUREMENT RESULTS AND PREDICTIONS

V. HONGISTO, J. KERÄNEN AND M. LINDGREN

Finnish Institute of Occupational Health, Laboratory of Ventilation and Acoustics, Lemminkäisenkatu 14-18 *B, FIN*-20520 *Turku, Finland*

(*Received* 20 *October* 1998, *and in final form* 23 *August* 1999)

In the first part of this paper the prediction models for both structural and leak transmission of doors were presented [1]. In this second part, results are presented for tested models comprising nine steel passage doors and nine timber passage doors. The results are presented in a form of two practical case studies. All measurements were made by the two-microphone sound intensity method. The structural SRI of a door was determined when the door was properly tape-sealed. The predicted structural R_w was on an average $1{\cdot}0 \pm 1{\cdot}5$ dB higher than measured R_w of tape-sealed doors, the range of variation being $-1 \ldots +3$ dB ($N = 13$). The average difference between the predicted and the measured SRI increased gradually with frequency from -3 up to $+12$ dB. The best structural solutions were those where two rigid panels formed a double panel without interpanel connections. The interpanel cavity was filled with sound-absorbing material which does not form rigid interpanel connections. Structures with previous descriptions were found to give 8–10 dB better values of R_w than structures comprising strong interpanel connections with the same mass. Gomperts' model for slit-shaped apertures predicted reasonably well the frequency behaviour of slit transmission when no seals were present (open apertures). When the door seams were sealed with rubber seals, the slits behaved in a more complex way probably because of the irregular shape of the slit. The total SRI of the door was calculated by the area-weighted sum of the predicted structural transmission and the predicted slit transmission. Approximating the slit transmission coefficient by Gomperts' model and predicting the structural transmission by Sharp's model produced a good overall prediction accuracy for the total SRI of the doors throughout the frequency range of interest.

1. MEASUREMENT METHODS

The arrangement of the measurement laboratory is shown in Figure 1. The measurements were carried out according to the principles of the new ISO/DIS 15186-1: 1998 using the sound intensity method and point-to-point measurements [2, 3]. The sound intensity method is very appropriate for testing of doors because the sound flow through the door, especially through the sound leaks, can be localized.

The source room was reverberant with a total volume of 80 m^3 ($7{\cdot}6 \times 2{\cdot}94 \times 3{\cdot}6$ m). The receiving room was anechoic with a total volume of 33 m^3

0022-460X/00/060149 + 22 $35.00/0

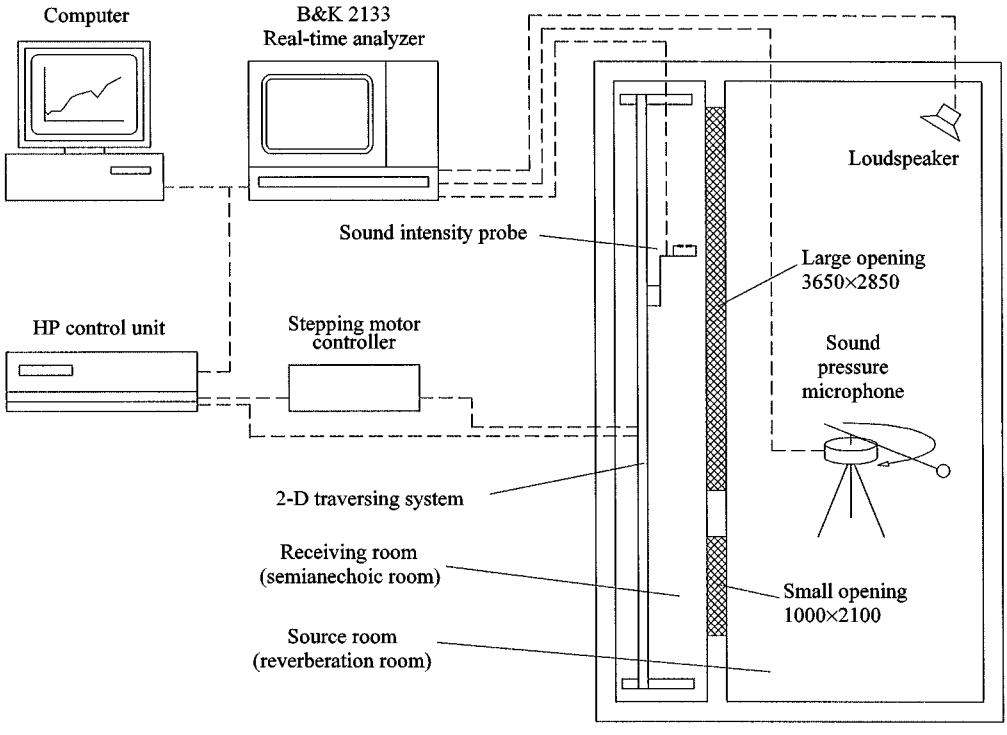

Figure 1. A schematic layout of the test laboratory and the measurement equipment.

($7{\cdot}6 \times 4{\cdot}0 \times 1{\cdot}1$ m). About 70% of the surface area of the receiving room was covered by 150 mm thick absorption material to reduce the reflections from the backwall close to the test object. The walls of the rooms were built of 160 mm thick concrete and the floor and ceiling was built of 265 mm thick hollow concrete. The junctions joining the individual rooms were not vibration isolated from each other. The space-averaged reverberation times of both rooms are given in Table 1.

The test signal was produced by a three-angular pyramid loudspeaker having one element on each of its surfaces. The radiation pattern of the loudspeaker was close to omnidirectional. The loudspeaker was fed with pink noise generator of the real-time analyzer (Brüel & Kjaer 2133). The sound pressure level in the source room was measured with a condenser microphone (Brüel & Kjaer 4165) mounted on a rotating microphone boom (Brüel & Kjaer 3923). The radius of rotation was 75 cm. There were three positions of the rotating boom, the averaging time being 32 s on each position.

The sound intensity was measured by using a sound intensity probe (Brüel & Kjaer 3545) provided with two 1/2″ phase-matched condenser microphones (Brüel & Kjaer 4181) mounted face-to-face. The spacer between the microphones was 12 mm allowing usually the frequency range 80–5000 Hz to be measured with an accuracy of $\pm 0{\cdot}5$ dB. The pressure-residual intensity indicator was determined in a calibration chamber (Brüel & Kjaer 3541).

The sound intensity probe was moved with a two-dimensional (2-D) traversing system providing an accuracy of 1 mm. The measurement surface and the probe

TABLE 1

The reverberation time of the source room (T1) *and the receiving room* (T2) *in* 1/1-*octave bands*

Octave band (Hz)	125	250	500	1000	2000	4000
T1 (s)	3·0	4·0	4·5	3·7	3·1	2·3
T2 (s)	0·3	0·2	0·2	0·2	0·1	0·2

were located at a distance of 12–18 cm from the specimen. The point-to-point measurement grid was usually 10–15 cm dense. The number of measurement points was 50–72 for usual door with dimensions 900×2100 mm. All intensity indicators of ISO/DIS 15186-1 and also ISO 9614-1: 1993 were monitored and the intensity measurements were arranged accordingly. Typical values of F_{pl} were in the range 0–7 dB being far below the dynamic capability of the sound intensity measurement system L_d. All sound signals were analyzed with the two-channel real-time analyzer (Brüel & Kjaer 2133).

The sound reduction index was determined by

$$R = L_{p,1} - L_{I,2} - 6 + 10 \log(1 + Sc/8Vf),$$

where $L_{p,1}$ (dB) is the average sound pressure level of the source room, $L_{I,2}$ (dB) is the average sound intensity level on the sound intensity measurement surface in the receiving room, c (m/s) is the speed of sound in air and f (Hz) is the middle frequency of the appropriate frequency band. The recommended values were used for the volume and boundary areas of the receiving room, $V = 81$ m^3 and $S = 117$ m^2.

2. CALCULATION METHODS

A calculation software (SRICALC) was developed based on the theories presented in reference [1]. The programming was accomplished by Visual Basic 3.0 software. The calculations were performed in 1/9-octaves at frequency range 50–20 000 Hz so that sufficient frequency resolution close to the discrete transition frequencies (f_{cr}, f_l, f_{br}, f_{mam}) could be achieved. The prediction results are presented in 1/3-octaves calculated from the average SRI of three 1/9-octave bands belonging to each 1/3-octave band. The error caused by discrete calculation is probably small because the spectrum is quite flat in 1/9-octave band scale.

The calculations for double panels were mainly done by using Sharp's model where the absorption inside the cavity is assumed to be high. This calculation is very straightforward as shown in equation (6) of reference [1]. When the absorbent was not present, equations (10) and (11) were applied. The diffuse sound transmission coefficient given by equation (11) was calculated by using numerical integration. The resolution of the sound incidence angle was $\mathrm{d}\theta = 0{\cdot}1^\circ$. The calculation was performed in 1/27-octaves instead of 1/9-octaves to avoid problems of discrete frequencies in enclosed spaces. Results were also presented in 1/3-octaves.

3. MATERIALS AND MOUNTING

Nine steel doors and nine timber doors were examined by measurements and predictions. The materials used are given in Table 2. The acoustical structures of timber doors and steel doors are described in Tables 3 and 4 respectively. One graphical example of both door sets is presented in Figures 2 and 3 including also the shape of the door frames, door leaves and the positions of rubber seals. The timber doors were mounted to a measurement opening of size $2100 \times 1000 \times 25$ mm (see Figure 1). The opening frames were made of 22 mm thick plywood attached tightly against the concrete wall separating the measurement rooms. The edges of the timber door frame were sealed with silicon gasket and/or air-conditioning tape.

The steel doors were mounted to the same measurement opening but the opening had to be narrowed by 230 mm. The narrowing structure was made of two chipboard panels of thickness 22 mm separated by an air cavity of 200 mm filled with sound-absorbing material. Preliminary measurements showed that the narrowing structure was sufficient to allow sound reduction index measurements up to $R_w = 50$ dB by using the pressure method ISO 140-3. By using the sound intensity method, even higher values of R_w could be measured because the narrowing structure does not belong inside the measurement surface.

A 50 mm wide air-conditioning tape was used for tape-sealing the sound leaks (apertures) of the doors. When single tape-sealing was applied, only one side (source room side) of the apertures was covered.

TABLE 2

Acoustical materials of doors and their abbreviations used in Tables 2 *and* 3

Abbreviation	Explanation
	Panel materials
HB	Hard board
CB	Chipboard
FB	Fibre board
S	Steel
PS	Steel with 25% perforated area
	Air cavity materials
AC	Air cavity
$n \times$ SL	n pieces of wooden support laths
$n \times$ SLF	n pieces of support laths having the edge covered by a flexible isolator
RW *xxx*	Rock wool, fibres perpendicular to door
RW *xxx*P	Rock wool, fibres parallel to door
xxx	Density of the rock wool in kg/m^3
	Glue descriptions
lg	Attachment by using lots of glue
rg	Attachment by significantly reduced amount of glue
ng	No glue

TABLE 3

The acoustical structures of the timber doors T1–T9; *mass is the total mass* (kg) *of the installed door*; *the material abbreviations are explained in Table* 2; *the material abbreviation is followed by thickness in* mm; *the structure drawing of the door* T1 *is given in Figure* 2

Timber doors (T1–T9): size 900 × 2000 mm			
Door label	Description of the structure	Mass	$R_{w,struct}/R_{w,total}$
T1	HB 3·2-lg-CB 6·0-lg-AC 27·5 with RW 150 26·0 and 6 × SL-ng-CB 6·0-lg-HB 3·2	40·9	36/33
T2	CB 6·0-ng-CB 6·0-AC 20·0 empty-CB 6·0-ng-CB 6·0	40·9	36/—
T3	CB 6·0-ng-CB 6·0-ng-AC 20·0 with RW 150 18·0-ng-CB 6·0-ng-CB 6·0	48·3	42/—
T4	HB 3·2-lg-CB 6·0-lg-AC 27·5 with RW 150 26·0 and 6 × SLF-ng-CB 6·0-lg-HB 3·2	46·0	36/—
T5	HB 3·2-lg-CB 6·0-lg-AC 32·0 with RW 150 32·0 and 6 × SL-lg-CB 6·0-lg-HB 3·2	48·0	32/
T6	HB 3·2-lg-CB 6·0-lg-AC 27·5 with RW 150 27·5 and 6 × SL-lg-CB 6·0-lg-HB 3·2	47·6	31/
T7	HB 3·2-rg-CB 6·0-rg-AC 27·5 with RW 150 27·5 and 2 × SLF-ng-CB 6·0-rg-HB 3·2	44·7	40/—
T8	CB 8·0-rg-AC 25·0 with RW 150 25·0 rg-HCB 3·2-rg-CB 6·0	37·0	40/39
T9	HB 3·2-lg-HB 3·2-lg-FB 11·0-lg-HB 3·2-lg-FB 11·0-lg-HB 3·2-lg-FB 11·0-lg-HB 3·2-lg-HB 3·2	58·0	40/—

TABLE 4

The acoustical structures of the steel doors S1–S9; *mass is the total mass* (kg) *of the installed door*; *the material abbreviations are explained in Table* 2; *the material abbreviation is followed by thickness in* mm; *the structure drawing of the door* S1 *is given in Figure* 3

Steel doors (S1–S9): size 730 × 2000 mm			
Door label	Description of the structure	Mass	$R_{w,struct}/R_{w,total}$
S1	S 0·75-lg-RW 220 20·0-AC 4·0 with one supporting RW 150P 4·0 (w = 100)-RW 220 20·0-lg-S 0·75	36·8	43/40
S2	S 1·0-lg-RW 220 20·0-AC 4·0 with one supporting RW 150P 4·0 (w = 100)-RW 220 20·0-lg-S 1·0	43·4	44/42
S3	S 0·75-lg-RW 220 20·0-lg-PS 0·5-AC 4·0 empty-PS 0·5-lg-RW 220 20·0-lg-S 0·75	43·7	47/43
S4	S 0·75-lg-RW 150 20·0-lg-S 0·75-ng-RW 150 20·0-lg- S 0·75	41·1	46/40
S5	S 0·75-lg-RW 220 20·0-lg-RW 220 20·0-lg-S 0·75	37·1	37/36
S6	S 0·75-lg-RW 150 42·0-lg-S 0·75	37·8	35/—
S7	S 0·75-lg-RW 220 20·0-lg-S 0·50-AC 4·0 empty-S 0·50-lg-RW 220 20·0-lg-S 0·75	44·0	39/39
S8	S 1·0-lg-RW 160 16·0-lg-RW 220P 15·0-lg-RW 160 16·0-lg-S 1·0	44·8	36/35
S9	S 1·0-lg-RW 220 15·0-AC 18·5 with 3 supporting RW 160P (w = 120)-RW 220 15·0-lg-S 1·0	41·1	45/39

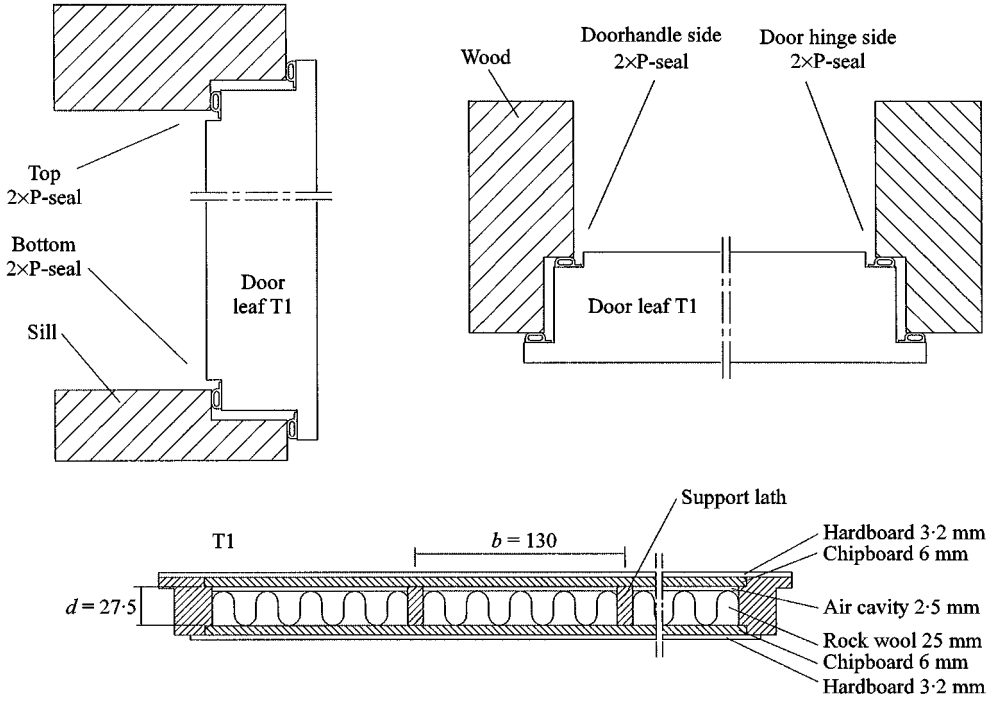

Figure 2. The timber door T1. Top left: side cross-section; top right: top cross-section. Bottom: the structure of the timber door T1 (see also Table 3).

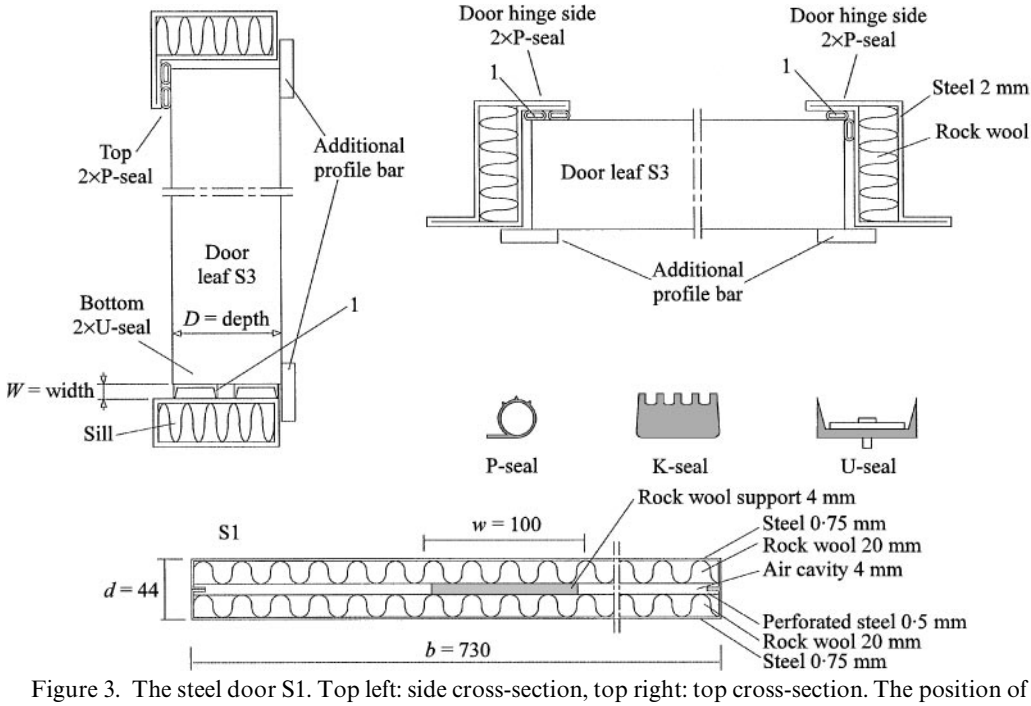

Figure 3. The steel door S1. Top left: side cross-section, top right: top cross-section. The position of the additional profile bar is indicated. Notation "1" means the position of the seal when single sealing was used. Middle: the shapes of the rubber seals used for steel doors. Bottom: the structure of the steel door S1 (see also Table 4).

4. RESULTS

4.1. TIMBER DOORS: STRUCTURAL EXAMINATION (SEE TABLE 3 AND FIGURE 4)

The development process started from the door T1 whose weighted SRI was to be increased by 3 dB. The stiffness of the door T1 was sufficient because of six vertical interpanel wood support laths. However, the support laths acted as strong sound bridges.

The highest stiffness was obtained by filling the air cavity completely by rock wool. All layers were glued together. This was realized for the doors T5 and T6 having 32 and 27·5 mm thick air cavities respectively. However, this solution yielded the worst overall result since both doors behaved acoustically like sandwich panels and the dilatation resonance frequency predicted by equation (18) covered the whole frequency range of interest above 800 Hz. The highest deviation from the mass law was even -18 dB which reflects the inferior sound insulation of sandwich structures.

The effect of cavity absorbent and its absence was tested for the doors T2 and T3. There were no support laths ($b = 900$ mm) and the highest possible value of $\Delta R_M = 11{\cdot}3$ dB could be achieved. (For comparison, $b = 130$ mm for the door T1 yielded $\Delta R_M = 2{\cdot}9$ dB.) The thickness of the air cavity was 20 mm. The door T2 was without the absorbent and the door T3 with 18 mm thick absorbent placed loosely throughout the air cavity. No glue was used between the panels and absorbent. The effect of the cavity absorbent is obvious (T2). When the cavity is empty the surface panels are effectively coupled together as if there were mechanical sound bridges. It behaves like a single panel with the same mass following mass law. When the absorbent is placed in the cavity (T3) almost perfect double-panel curve with $b = 900$ mm is obtained. At high frequencies, the overestimation of the predicted value is most probably due to the critical frequency of the individual chipboard panels. Sharp's model does not respond to the behaviour of bridged double panels at and above the critical frequency of individual single panels.

The effect of support laths was studied also by placing elastic material (P-type seal as presented in Figure 3) on the lath to obtain flexible contacts between the lath and surface panel (T4). The thickness of the support laths was reduced by the thickness of the elastic material respectively. The periphery frame of the door was not modified to maintain the stiff basic structure of the door. All other properties were similar to the door T1. The transmission via the laths was assumed to reduce by using flexible support laths. An additional dip appeared at 400 Hz of the door T4 which may be due to a new mass–spring–mass resonance. The spring is the elastic material on the lath instead of air. The rapid rise of SRI above 400 Hz is typical behaviour for double panels. The weighted SRI did not increase by the flexible material of this kind.

Finally, the effect of reducing the amount of glue on the panel–panel and absorbent–panel interfaces was examined. The effect is seen on the behaviour of the doors T7 and T8. No sandwich-type dilatation resonance frequencies can be seen although the air cavity is completely filled with absorbent like the doors T5 and T6. The door T7 was accomplished by placing only two support laths with flexible contacts out of six to increase the value of ΔR_M. The high-frequency insulation of door T7 is the highest of the whole timber door series. The door T8 was

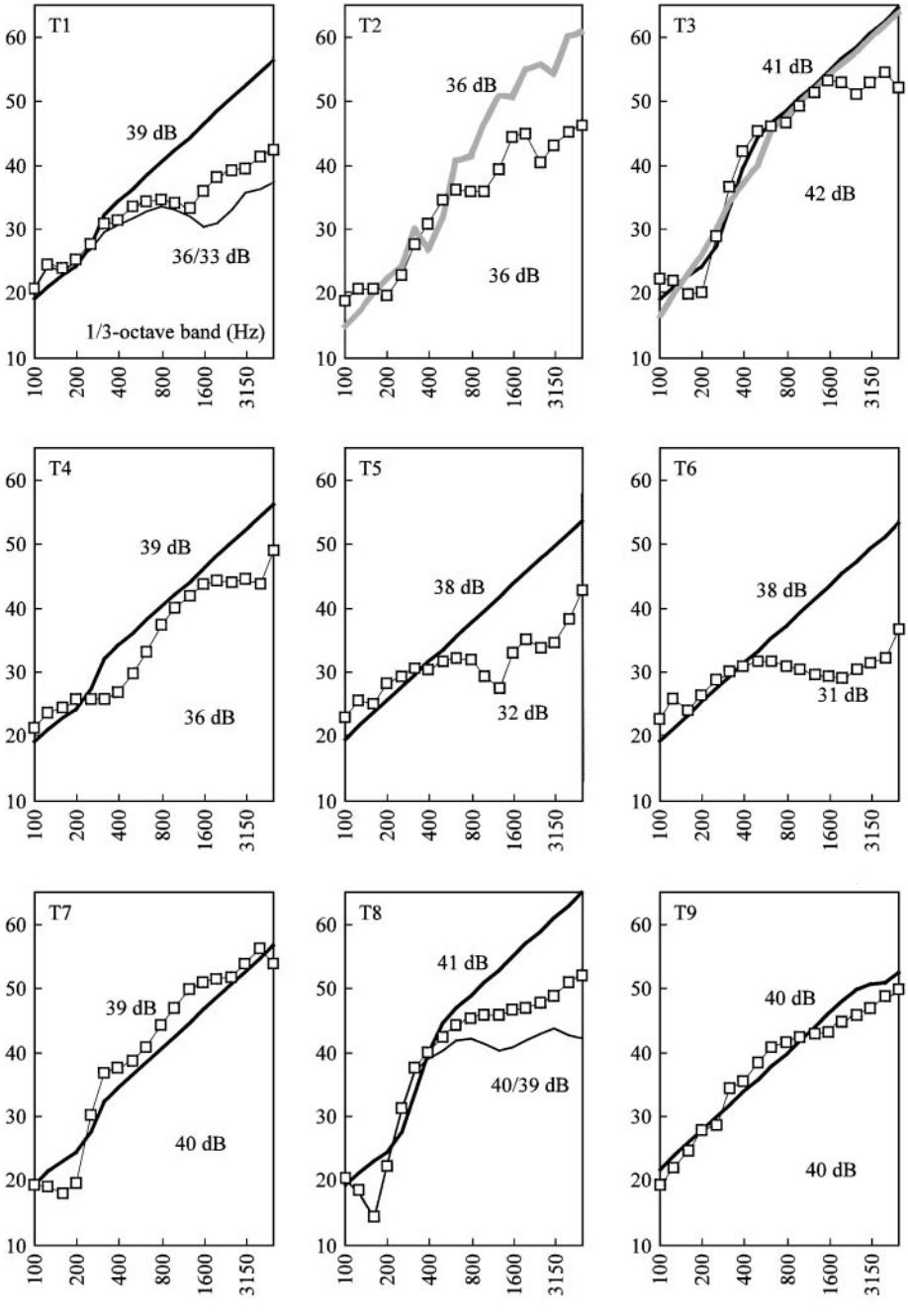

Figure 4. The measured and predicted SRI of the timber doors T1–T9 at 1/3-octave frequency bands 100–5000 Hz. All doors were properly tape-sealed. Grey line is obtained by equations (10) and (11) and black line by equation (6) of reference [1]. Interpanel connections were considered in each case by equations (14) and (15). The upper number value in each graph is the predicted R_w and the lower number value is measured laboratory performance $R_{w,struct}/R_{w,total}$: ——, R_{total}, measured, slits not sealed; —□—, R_{struct}, measured, slits sealed; ——, R_{struct} calculated, slits sealed, absorbing cavity; ▬, R_{struct} calculated, slits sealed, empty cavity.

accomplished without support laths and reduced the amount of glue but the panel structure was changed a little.

The door T9 is completely different from the doors T1–T8. Its structure comprises 9 panels and 8 glue layers. This door was selected for this study to show that the mass-law works reasonably well for glued multilayer structures.

Measured and predicted results for timber doors are presented in Figure 4. Double-panel theory was applied to the doors T1, T3, T4, T7 and T8 by equation (6) [1]. The double panel formed by one 6·0 mm thick chipboard and one 3·2 mm thick hardboard without air cavity was obtained by equation (17). The absence of the cavity absorbent for the door T2 was obtained by equations (10) and (11) [1]. This curve is printed with a grey solid line. The absorption coefficient of the door T2 was $\alpha = 0{\cdot}05$ and the width of the free space in the cavity was $S = 900$ mm. For comparison, the door T3 was modelled both by equations (6) and (10), (11). The absorption coefficient of the door T3 was $\alpha = 0{\cdot}95$. This value was taken from the absorption coefficient data above 500 Hz. The width of the free space in the cavity was $S = 900$ mm. The interpanel coupling was considered in each case by equations (14) and (15) [1].

The doors T5 and T6 were considered to be sandwich constructions since the rock wool which filled completely the air cavity was glued tightly on both surfaces to the wooden panels. The dilatation resonances were calculated according to equation (18) [1]. For the door T5 it was $f_d \approx 1470$ Hz with $m_1 = m_2 = 8{\cdot}7$ kg, $E_c = 3 \times 10^6$ N/m^2 and $t_c = 0{\cdot}032$ m, and for the door T6 it was $f_d \approx 1590$ Hz with $t_c = 0{\cdot}0275$ m. The measured shift of the dilatation resonance dip from the door T5 to the door T6 was larger than calculated when the thickness of the core changed from 32 to 27·5 mm. Also the shape of the dips changed from dual dip (T5) to a wide single dip (T6). This behaviour could not be explained.

4.2. TIMBER DOORS: LEAK EXAMINATION

The original door T1 and the structurally improved door T8 were studied. An example of the advancement of leak transmission versus structural transmission is presented in Figure 5. The laboratory performance of the original door T1 was 36/33 dB. The aim was to obtain $R_w = 39$ dB, or $\Delta R_{aim} = 3$ dB as explained in previous sections. It can be seen that for the door T1 the strongest sound leaks occurred above 1000 Hz, the maximum difference between the total SRI and structural SRI being $\Delta R = 7{\cdot}1$ dB at 2000 Hz. Coincidentally, the maximum unfavourable deviations from the $R_w = 31$ dB curve (according to ISO 717-1) occurred at 1000–2500 Hz. According to equations (3) and (4) [1] the value $R_w = 39$ dB cannot be achieved solely by structural changes of the door leaf.

The structurally improved door T8 is presented in Figure 5 (labelled $R_{total,T8A}$) without changes in the sealing. The structural sound insulation was obtained by reducing the mechanical connections between the panels as explained in the previous section. The improvement of the structure did not increase R_w. When the sealing of the door was improved from T8A to T8B, an increase by 4 dB could be obtained in $R_{w,total}$ and the final laboratory performance of the door was 40/39 dB.

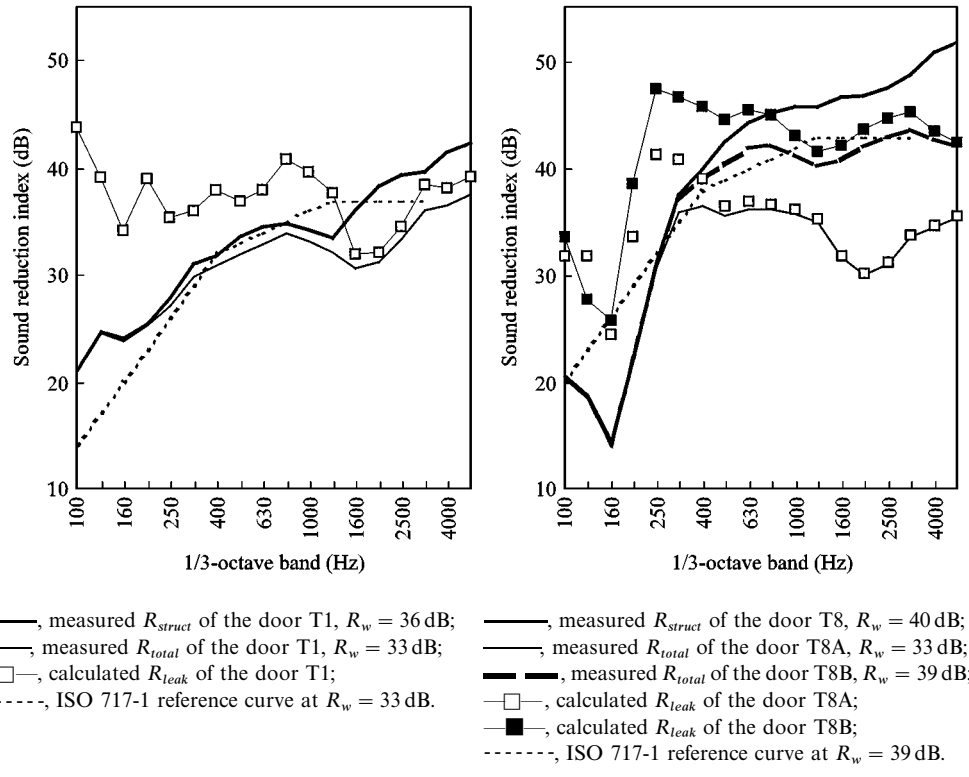

Figure 5. The sound reduction index of the original timber door T1 (left) and the developed timber door T8 (right). R_{leak} was calculated by equation (2) of reference [1]. R_{struct} is the tape-sealed SRI where sound leaks are eliminated. R_{true} is the normal SRI of the door including sound leaks.

The sealing improvements were obtained by a certain double P-type rubber seals instead of single P-seals.

The leak sound reduction index R_{leak} calculated by equation (2) of reference [1] is presented in Figure 5. (Note that R_{leak} in equation (2) represents the SRI of the leaks averaged over the area of the door and not the SRI of the leak area.) All three cases, T1, T8A and T8B were calculated. The change of $R_{leak,\,T1}$ was negligible compared to $R_{leak,\,T8A}$ as expected because no changes were made on the sealing of the door. But when the sealing was improved, the leak SRI ($R_{leak,\,T8B}$) increased by 6–14 dB above 1000 Hz. The total SRI of the door increased correspondingly by 5–12 dB from $R_{total,\,T8A}$ to $R_{total,\,T8B}$. That is to say, the improvement in sealing reflected directly to the total SRI of the door because the structural SRI was much higher than the leak SRI.

The values of $R_{leak,\,T1}$ and $R_{leak,\,T8A}$ should be equal because no changes were made in rubber sealing. However, there are major differences at low frequencies. The difference is likely to be due to poor repeatability of the measurement method at low frequencies. Equation (2) of reference [1] is very sensitive to small values of ΔR. For instance, if the structural (tape-sealed) SRI is $R_{struct} = 30$ dB and $\Delta R = 0{\cdot}1$ dB one gets $R_{leak} = 30$ dB. Therefore, high values of R_{leak} should be considered with reservations.

4.3. SUMMARY OF TIMBER DOORS

The laboratory performance of the original door T1 having $R_{w,struct}/R_{w,total} = 36/33$ dB could be developed to the new door T8 having $R_{w,struct}/R_{w,total} = 40/39$ dB. The reduction of interpanel connections (glue and support laths) was the key point for structural improvements. The compromise between good stiffness and good sound insulation could be found by replacing six original laths by two laths with elastic contacts. Sandwich solutions like those presented in this section cannot be used when good sound insulation and low weight is required. The sealing improvements could be obtained with carefully placed double P-type seals. Without sealing improvements the improvement would have been only 2 dB instead of the obtained improvement of 6 dB.

For the developed door T8, the unfavourable deviations from the ISO 717-1-curve occur in turn at low frequencies near the mass–air–mass resonance frequency $f_{mam} = 160$ Hz. For the original door T1, the unfavourable deviations occurred at high frequencies. Therefore, it can be concluded that further development of the door needs simultaneous improvement of sealing and increasing the total mass.

4.4. STEEL DOORS: STRUCTURAL EXAMINATION (SEE TABLE 4 AND FIGURE 6)

The development process started from the door S1 having laboratory performance $R_{w,struct}/R_{w,total} = 43/40$ dB. The weighted SRI needed to be increased by 3 dB to $R_{w,total} = 43$ dB. Also the stiffness of the door needed to be increased.

The first structural improvement of the door S1 was made by increasing the mass of the surface panels from 0·75 to 1·00 mm (S2). The door S9 was also accomplished by thick surface panels, and, in addition, the thickness of absorbents was increased. The change of $R_{w,struct}$ was 1 dB from the door S1 to the door S2 both by measurements and by calculations. Surprisingly, the change of the absorbents for the door S9 caused an additional increase of SRI by 1 dB. Probably, the thickening of the soft support absorbent strips inside the air cavity reduced the bridging through the core.

However, increasing the thickness of the surface layers was not desirable for several practical reasons. The optimum thickness was 0·75 mm for the surface panel. Therefore, other methods should be found to improve the sound insulation.

On the basis of the difference between doors S1 and S9 it was concluded that the support absorbents should be removed. The reduction of the stiffness caused by this was to be compensated in some other way. The mass of the surface panel was increased by placing additional steel panels inside the cavity so that two thin sandwich panels of thickness 20 mm were formed. They were separated by a 4 mm thick air cavity (S7). However, this structure was not a good solution because the air cavity of thickness 4 mm acted as an air spring causing a strong mass–air–mass resonance at 400 Hz band.

When both additional steel panels in the cavity were perforated (S3), the desired increase of the structural SRI was obtained. In addition, the stiffness of the door S3 was remarkably higher than that of door S1. Sound waves could escape from the

4 mm cavity through the perforated panel to the mineral wool. The thickness of the cavity increased from 4 mm (S7) to 45 mm (S3).

Also inexpensive structures were under investigation. Good stiffness and simple manufacturing process could be attained by sandwich structures. Three different versions were investigated. The worst overall result was obtained with door S8 having the highest mass of the whole steel door series. The middle layer of three rock wool layers was much softer than the other layers (lowest Young's modulus). The spring formed by the core became more loose but, however, stiff enough to produce a strong dilatation resonance frequency at 500–630 Hz. Other sandwich doors were accomplished by one (S6) or two (S5) identical rock wool layers and the dilatation resonances were at 4000 and 2500 Hz, respectively.

One modification between the sandwich panels and the double panels was the door S4. One steel panel in the middle was glued from one side to the adjacent rock wool. The other side of the middle steel panel was not glued so that sandwich-type sound bridges were not formed on that side of the panel. The overall result $R_w = 46$ dB was encouraging since the manufacturing of this structure was very simple, the only acoustical secret being the glueing on one side. The thin sandwich panel formed by the middle panel and the other surface panel did not cause dilatation resonances at the frequency range of interest because the thickness of the mineral wool was only 20 mm. Problematic sandwich doors S5, S6 and S8 had mineral wool thickness above 40 mm.

The measured and predicted results for the steel doors are presented in Figure 6. The calculations were made according to reference [1] as in Figure 4. The doors S1, S2, S3, S4, S7 and S9 were considered as double panels. The doors S5, S6 and S8 were considered as sandwich constructions since the rock wool, which filled completely the air cavity, was glued tightly on both surfaces to the surrounding steel panels. In this case, the thickness of the air cavity was within $d = 40$–50 mm except door S7 with $d = 4$ mm. Thin cavity shifted the mass–air–mass resonance frequency from typical value $f_{mam} = 160$ Hz up to 400 Hz. The steepness of the slope right above f_{mam} reveals the double-panel behaviour for all double panels. Also the bridging frequency f_{br}, where the steep upward slope is cut due to line-type sound bridges, is evident. The dilatation resonances occur for the doors S5, S6 and S8 at frequencies 4000, 2500 and 500 Hz, respectively. The depth and the width of the resonance dips change considerably. Simple mass-flow prediction was used in the absence of a suitable sandwich prediction model.

4.5. STEEL DOORS: LEAK EXAMINATION

The shape of the steel door leaf was very simple as shown in Figure 3. The total SRI of the door was very sensitive to sealing. Therefore, the proper shape of the seal, the door frame and the door itself were very valuable for the overall performance.

The properties of good seals are, firstly, to cover the clearances between the door and frame completely without a need to use excessive force in operation (good fitting), secondly, to have a sufficient sound insulation in itself to prevent sound transmission through the seal, and, thirdly, to have good

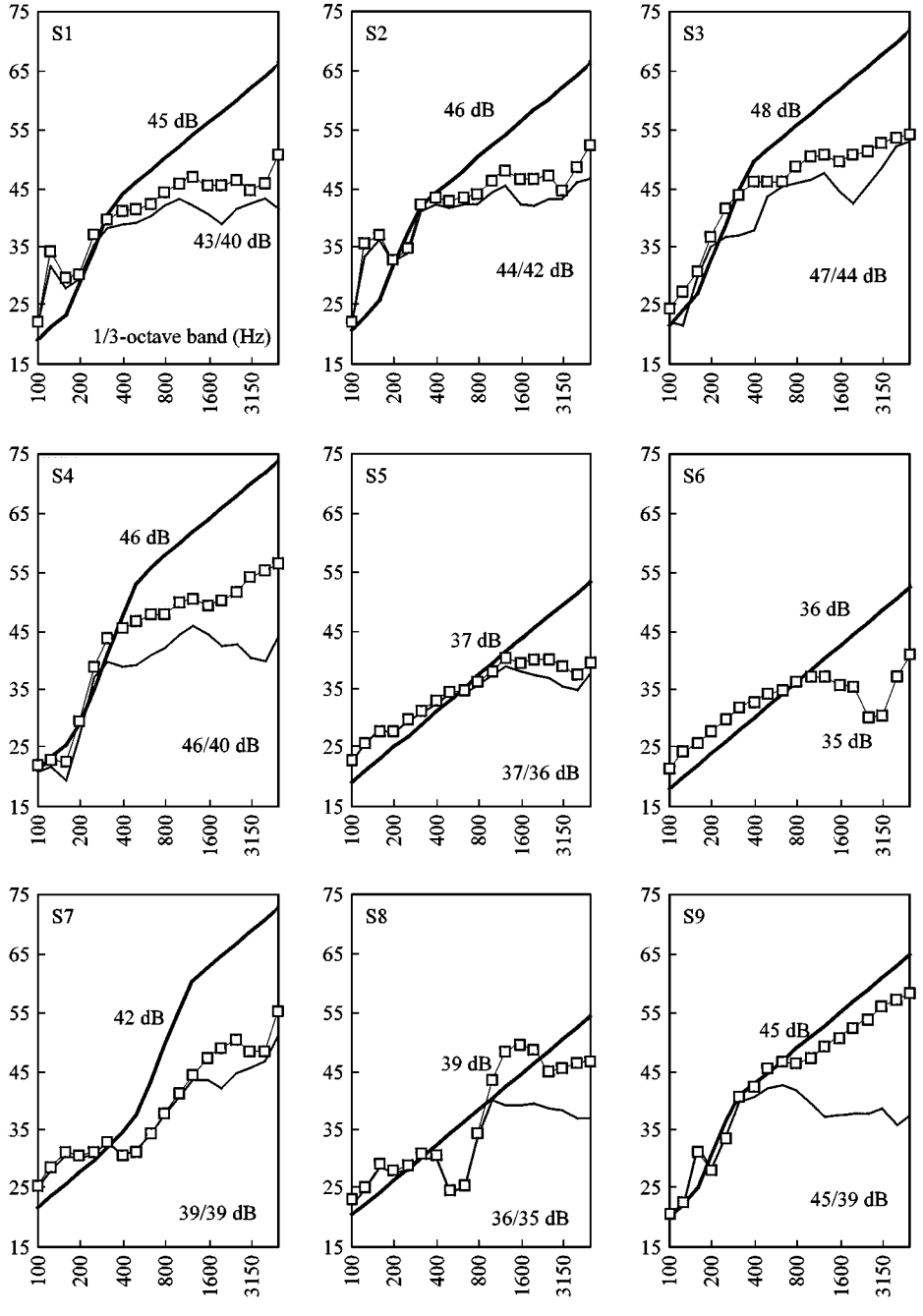

Figure 6. The measured and predicted SRI of the steel doors S1–S9 at 1/3-octave frequency bands 100–5000 Hz. All doors were properly tape-sealed. The upper number value in each graph is the predicted R_w and the lower number value is measured laboratory performance $R_{w,struct}/R_{w,total}$: ——, R_{total}, measured, slits not sealed; —□—, R_{struct}, measured, slits sealed; ——, R_{struct}, calculated, slits sealed, absorbing cavity.

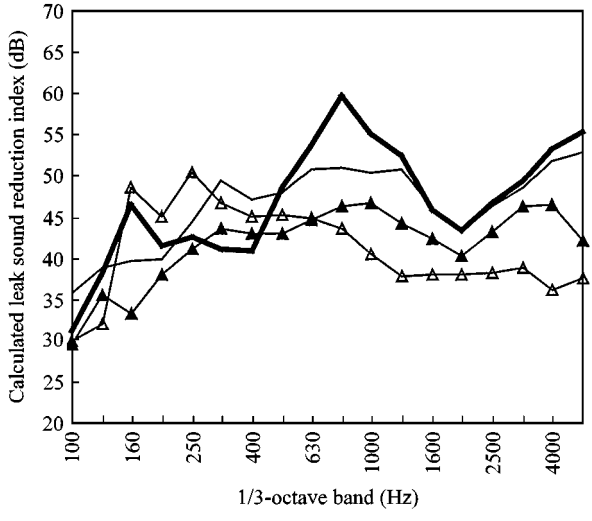

Figure 7. The leak sound reduction index of steel doors calculated according to equation (2) of reference [1]. S9: K-seal, S1: P-seal, S7: P-seal and U-seal on the bottom, S3: as S7 but the clearance between the door and frame was made uniform around the door. The shapes of the seals were elucidated in Figure 3: —▲—, R_{leak} of the door S1; ——, R_{leak} of the door S3; ——, R_{leak} of the door S7; —△—, R_{leak} of the door S9.

durability. P-type and U-type rubber seals presented in Figure 3 were studied in this section.

The calculated leak sound reduction indexes of the doors S1, S3, S7 and S9 are shown in Figure 7. (Note that R_{leak} in equation (2) represents the SRI of the leaks averaged over the area of the door and not the SRI of the leak area.) The calculation was made according to equation (2) of reference [1]. The sealing of the first door S1 was accomplished by a double P-type seals. The problem was the poor durability of the seal against the bottom sill. Therefore, thick K-type seals were selected for door S9. However, the leak transmission was very strong. The fitting of the K-type seal was found poor.

Finally, a U-type seal was used against the bottom sill and a P-type seal was used in other clearances. This construction was used for door S7 with good results. Transmission via the bottom sill was fully eliminated. A U-type seal fits best to clearances where the seal slides against the frame.

After the seals were properly selected, it appeared that the door did not fit properly to its frames. The clearances were not uniform around the door. The manufacturing dimensions of the door were changed and the door S3 was obtained with highest laboratory performance $R_{w,struct}/R_{w,total} = 47/44\,\text{dB}$.

4.6. EFFECT OF DIFFERENT SEALING CONDITIONS ON THE STEEL DOOR S3

On the basis of the work made on sealing the door S3, it was concluded that there is probably no other means to reduce the leak sound transmission than to change the shape of the door leaf by using a profiled door leaf to hinder the sound

transmission in the apertures. Therefore, a systematic test procedure was carried out to examine the effect of different sealing conditions on the total sound insulation. A steel door with high structural sound insulation was selected (S3) to be able to detect smallest possible sound leaks.

The sealing factors to be varied were as follows: rubber sealing: single sealing (rs1), double sealing (rs2) or no sealing (rs0); tape sealing: one side of the door only (ts1), both sides of the door (ts2), or no tape-sealing (ts0); additional profile bar sealing: with (pb1) or without (pb0).

The profile bar, tape sealing and rubber sealing are described in Figure 3.

Ten measurement results with different combinations of sealing factors are given in Figure 8. The range of R_w was extremely wide: 24–46 dB. The effect of sealing was evident at high frequencies. At low frequencies the results are almost independent of sealing factors. These are two exceptions to that, namely doors without any rubber or tape sealing.

The effect of tape sealing is evident. Single tape sealing is not sufficient for eliminating sound transmission through slits when good sound insulating doors, like S3, are investigated. It is possible that even double-sided tape sealing is not sufficient to eliminate completely sound leaks but no other simple means could be found for the elimination of leaks.

Two P-type seals side-by-side instead of one P-type seal increased the total sound insulation. The hollow space inside the P-seal is obviously the reason for the good capability to shape against the door.

The effect of the additional profile bar increases with decreasing amount of rubber or tape sealing. The assumption that any obstacle covering the slit, like a profile bar, would decrease sound transmission remarkably was not right. The effect of the profile bar was only 1 dB with double rubber seals. When also tape seals were installed, no difference could be observed without the profile bar. (In fact, the result was poorer with the profile bar and double seals because the door did not shut properly anymore.)

The positions of high-frequency dips in Figure 8 are not fixed as would be expected. Their character is discussed later in this paper.

4.7. SUMMARY OF STEEL DOORS

The laboratory performance of the original door S1 with a performance $R_{w,struct}/R_{w,total} = 43/40$ dB could be developed to door S3 with a performance $R_{w,struct}/R_{w,total} = 47/44$ dB. The reduction of interpanel connections (mineral wool supports) and the increase of the mass were the means of structural improvements. Sandwich solutions are not recommended when good sound insulation and low weight is required. However, as the S4 proved, the sandwich structure can be modified very easily to a double panel, for example by removing one layer of glue which prevents the transmission of shear forces through the structure.

The sealing improvements could be obtained with two different double seal types in different seams. Without sealing improvements the true improvement

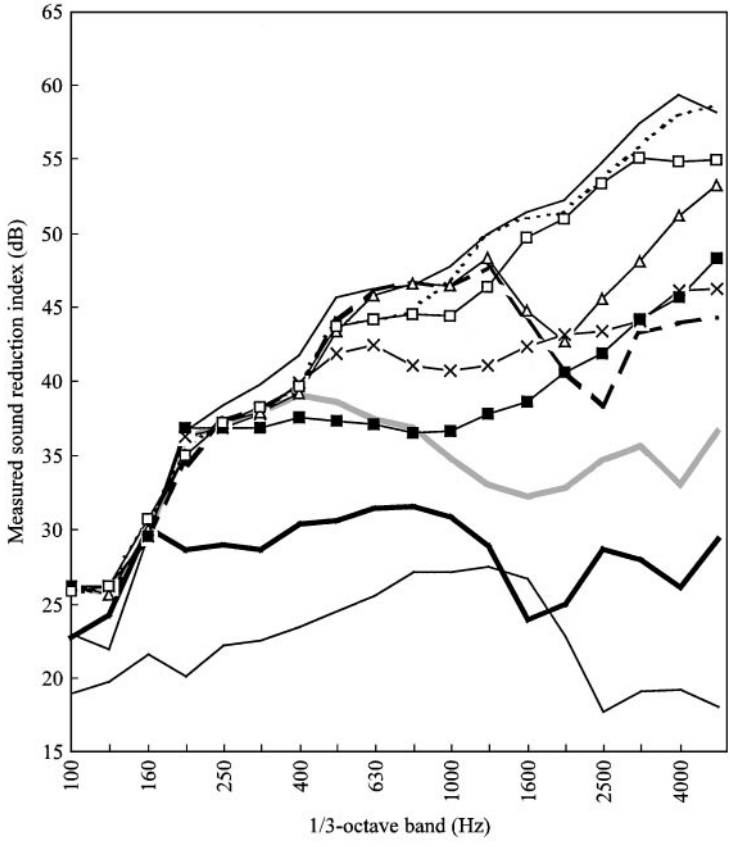

Figure 8. Sound reduction index of the steel door S3 with different sealing conditions. The weighted sound reduction index R_w is the last number of the label text. Labels: rs = rubber sealing, ts = tape sealing, pb = additional profile bar. Numbers 0, 1 or 2 right after the label express the number of sealings.

ΔR_{true} would have been 0 dB instead of 4 dB obtained as calculated by equation (4).

It seems that for a single door without profile bars, a laboratory performance like $R_{w,struct}/R_{w,total} = 50/50$ dB is very difficult to achieve even under laboratory conditions and by careful mounting. The door and frame profiles have to be designed to fit together properly and, if possible, the cavity inside the clearance should be sound absorbing. Also the lock plunger should be designed to tighten the door from the top and bottom. One plunger in the middle causes strong sound leaks on the corners, especially for timber doors as they have usually a more flexible leaf than steel doors. Above $R_w = 50$ dB single leaf doors may be difficult to handle because of great mass, as well.

4.8. THE VALIDITY OF THE DOUBLE-PANEL PREDICTION MODEL

To draw conclusions about the validity of the prediction model, it is necessary to know how accurately average predictions for this model can apply to the door constructions. The average deviation between the predicted and measured SRI is presented in Figure 9 for both timber and steel doors. All doors were properly tape-sealed. The minimum deviation, the maximum deviation and the standard deviation are also presented.

Sharp's double-panel theory was found reasonable for predicting the structural transmission of door leaves. The average overestimate of weighted sound reduction index R_w was only $1{\cdot}0 \pm 1{\cdot}5$ dB. At high frequencies the overestimations are obvious. The average overestimate increased gradually with increasing frequency from $-2{\cdot}8$ to $+11{\cdot}9$ dB. No obvious frequency dependence could be detected for the standard deviation, which was in the range 1·8–6·8 dB.

There may be several reasons to the overestimations. Some of them are given below.

As noted previously, even double-sided tape sealing may be insufficient to completely eliminate the sound transmission through sound leaks. However, any better practical sealing methods could not be found which were as quick and as simple to carry out. There are some examples, like the door S9, where the measured and predicted sound insulation are very close to each other and the SRI is rather high. Therefore, it is concluded that the transmission through the tape is not the only reason for the overestimated prediction results.

Resonant transmission below the critical frequency is not well considered in this study. The radiation of edge and corner modes is very strong and mass law is not sufficient to explain the transmission through small bounded specimen especially at low frequencies.

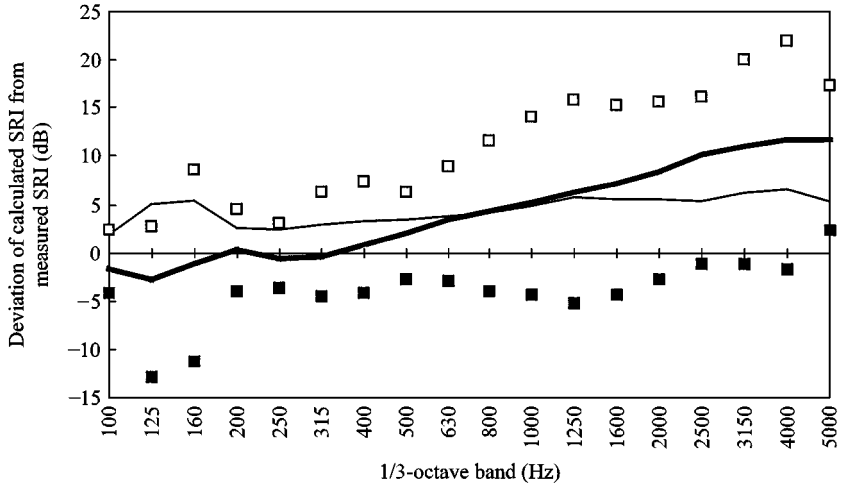

Figure 9. The maximum, minimum and average deviation of predicted SRI from measured SRI. All doors were properly tape-sealed. In all 13 double-panel doors, T1, T2, T3, T4, T7, T8, T9, S1, S2, S3, S4, S7 and S9 were included from Figures 4 and 6. Sandwich panels T5, T6, S5, S6 and S8 were omitted: ——— , average; ■, minimum; □, maximum, ——— , standard.

For steel doors, the narrowing structure of the measurement opening (filler wall) may have radiated sound to a certain degree because a part of it belonged inside the measurement surface. However, one measurement result was obtained with high values of SRI at high frequencies (S9). Therefore, it is likely that the door frame or frames of the measurement opening did not spoil measurement results systematically, since the measurement arrangements and the door frame were almost identical for each steel door.

Sharp's double-panel prediction model does not respond to the usual case where the critical frequency of individual panels belongs to the range where the sound transmission via the interpanel connections is the major sound transmission path through the air cavity. The model states that the value of ΔR_M is added to the value of R_M by equation (5a) [1]. The value of R_M could be obtained by equation (17). In this equation, both the non-resonant and the resonant contribution (critical frequency dips) of individual single panels are taken into consideration. This arrangement could have been affected the results obtained with timber doors having critical frequency below 5000 Hz. Because the development of the SRI-prediction models is not the primary aim of this study, this problem remains open.

The variations in the manufacturing process and mounting have also an affect on the sound reduction index. This effect could be studied for the doors T1 and S3. Both door prototypes were manufactured and tested three times during the project that lasted one year. The tests were made on tape-sealed doors. The minimum and the maximum differences in the SRI were calculated for each 1/3-octave frequency band. For steel doors, the average difference was 3·5 dB and the range was 0·3–5·6 dB. For timber doors, the average difference was 1·6 dB and the range was 0·7–2·8 dB. No frequency dependence was observed, which also justifies that the measured differences are not solely due to different measurement arrangements. The measurement uncertainty usually increases with decreasing frequency. The changes are quite small compared to the overall measured SRI changes during this study. Therefore, the conclusions drawn in the previous sections are justified. (In general, a much more probable source of specimen variations may be the misunderstandings in the chain researcher—production manager—worker. Information breaks in this chain have been observed many times when new door structures have been designed.)

Transmission through the door frames was ignored in this study for simplicity. The radiation of the frames would not have been simple to determine even with sound intensity method because of adjacent sound leaks. Fortunately, the surface mass of the timber or steel frame was always 2–3 times larger than the mass of the door leaf.

4.9. MODELLING OF THE SLITS AND THE TOTAL SRI OF THE DOOR

In this section, the total sound insulation of doors is predicted by using separate models for structural transmission and transmission through slits. The prediction results for the structural transmission were presented in previous sections. The modelling of slits is approached here by using two different models: Gomperts' model for slit-shaped apertures and Jones' model for irregular apertures.

The sound reduction index of an aperture that is typical for doors was presented in Figure 6 of reference [1]. The area of the door S_{door} and the area of slits S_{slit} are needed for the prediction of the total SRI. The total SRI was obtained by equation (19) of reference [1] where the value of R_{slit} was obtained either by equation (20) of reference [1] in the case of Gomperts' model or by using $R_{slit} = 0\,\text{dB}$ in the case of Jones' model. Both models were tested for two different sealing conditions of the door S3.

The first example is shown in Figure 10 without rubber seals, without tape sealing and without profile bar (see rs0 to ts0 pb0 and $R_w = 24\,\text{dB}$ presented in Figure 8). The Gomperts' model seems to work reasonably well. The predicted position of the slit resonance occurs at the frequency range where the minimum values of SRI are measured, although no evident slit resonance dip was found in measured results. Jones' model gives too low values below the lowest slit resonance frequency 3150 Hz while Gomperts' model gives good predictions throughout the frequency range.

A more practical example is shown in Figure 11 where the same door S3 is mounted with single rubber seals (rs1 ts0 pb0, and $R_w = 43\,\text{dB}$). In this case, the total transmission comprises structural transmission, slit transmission through free slits and transmission through the rubber seals. The area of the free aperture area S_{slit} is difficult to measure because of the rubber seals covering most of the apertures, therefore it is obtained by trial. The transmission through the rubber

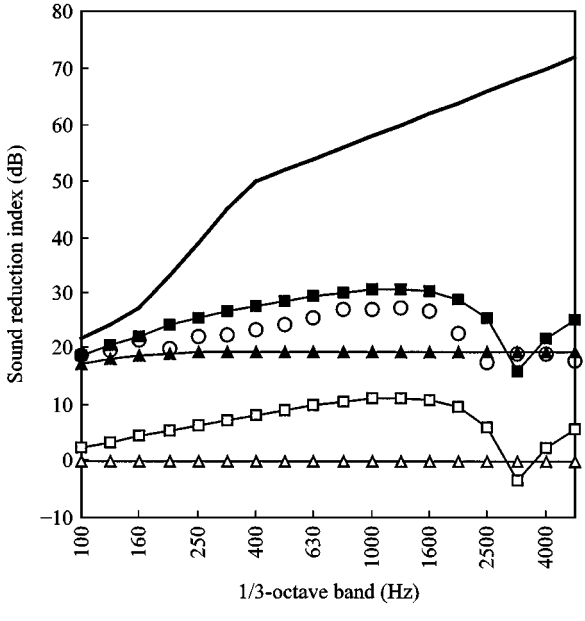

Figure 10. The predicted total SRI of the door S3 by equation (19) of reference [1]. No sealing was present in the door seams (see case rs0 ts0 pb0, $R_w = 24\,\text{dB}$ in Figure 8). The measured areas were $S_{slit} = 0{\cdot}0165\,\text{m}^2$ and $S_{struct} = 1{\cdot}43\,\text{m}^2$. The dimensions of the slit were $W = 2\,\text{mm}$ and $D = 45\,\text{mm}$: ——, calculated R_{struct}; —□—, calculated R_{slit} by Gomperts' model, $w = 2\,\text{mm}$; —■—, calculated R_{total} by Gomperts' model; —△—, calculated R_{slit} by Jones' model; —▲—, calculated R_{total} by Jones' model; ○, measured R_{total}.

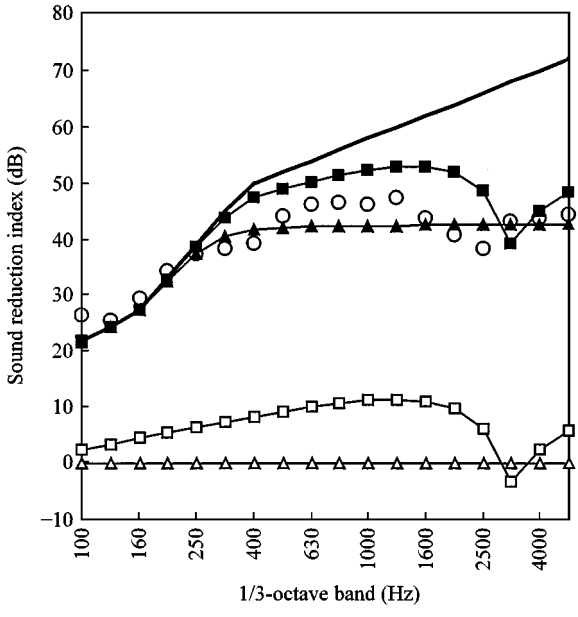

Figure 11. The predicted total SRI of the door S3 by equation (19) of reference [1]. Single rubber seals were used in the door (see case rs1 ts0 Pb0, $R_w = 43$ dB in Figure 8). The areas used in the calculations were $S_{slit} = 0{\cdot}00008\,m^2$ (best guess) and $S_{struct} = 1{\cdot}43\,m^2$. The dimensions of the slit were $W = 2$ mm and $D = 45$ mm: ——, calculated R_{struct}; —□—, calculated R_{slit} by Gomperts' model, $w = 2$ mm; —■—, calculated R_{total} by Gomperts' model; —△—, calculated R_{slit} by Jones' model; —▲—, calculated R_{total} by Jones' model; ○, measured R_{total}.

seals is not considered. The ideal behaviour of the slit-shaped aperture is assumed to disappear because the rubber seals have changed the acoustical edge conditions in the slit. In Figure 11, the shape of Gomperts' curve is conforming to the theory below the slit resonance frequency but the position of the calculated slit resonance is not correct. There are no simple logical explanations to the positions of slit resonances when the slits are sealed. Jones' model gives better results for sealed slits (see Figure 11) than for free slits (see Figure 10) because the ideal shape of the slit SRI has become less severe. It should be mentioned once again that the area of the slit S_{slit} in Figure 11 is not based on physical measurements as in Figure 10. The value $S_{slit} = 0{\cdot}00008\,m^2$ was the best guess.

Burgess found also Gomperts' slit theory inadequate to explain the reductions of SRI of windows at certain frequencies [4]. It was found on the basis of the casement dimensions that Helmholtz resonances can occur between the slit and the small volume inside the casement. This kind of explanation could not be thought to be relevant here because the cross-section of the slits are regular for the doors in this study.

5. CONCLUSIONS

1. The laboratory performance of a timber door could be improved from $R_{w,struct}/R_{w,total} = 36/33$ dB to 40/39 dB. The improvement of the acoustic structure

was obtained by reducing the amount of the wood support laths (interpanel connections), covering the surface of the support laths by a flexible material and by reducing the amount of glue between the surfaces. Correspondingly, the laboratory performance of a steel door could be improved from $R_{w,struct}/R_{w,total} = 43/40$ to 47/44 dB. The improvement of the acoustic structure was obtained by reducing the interpanel connections, as well, and by increasing the mass of the panels.

2. The theory presented in reference [1] for estimating the influence of structural or sealing improvements on the total sound reduction index of a door worked well in practice. Structural improvements of a door were not efficient if the sound leaks were not completely eliminated. As an example, if the difference of SRI between tape-sealed door (no sound leaks) and normally mounted door is above 3 dB, structural improvement by N dB leads to an improvement in total SRI that is below $N/2$ dB. Often much effort is wasted on structural improvements.

3. Sharp's double-panel theory was found to be a good tool for predicting the structural transmission of door leaves comprising double panels. The average difference between the predicted R_w and measured R_w was $1{\cdot}0 \pm 1{\cdot}5$ dB based on 13 specimens. The range was -1 to $+3$ dB. The standard deviation of the difference between the predicted and the measured SRI was in the range 1·8–6·8 dB but no clear frequency dependency could be observed. The average overestimate increased gradually with increasing frequency from $-2{\cdot}8$ to $+11{\cdot}9$ dB. Several reasons were listed for this behaviour. It is possible that the double tape sealing does not obstruct sound transmission through apertures perfectly, as was assumed. Also the small size of the door specimen (usually 900×2000 mm) may give rise to some factors that the present models do not consider. Sound transmission through the frames of the door were not modelled either although the frames included inside the measurement surface. It should be noted that strong overestimations at high frequencies is almost a rule for all prediction models.

4. It was found for six different sandwich-type doors that sandwich structures are acoustically very poor. Simple mass law prediction by equation (5a) was used for modelling sandwich-type doors. The average difference between the predicted R_w and measured R_w as $3{\cdot}0 \pm 3{\cdot}1$ dB based on 5 specimens. Typically, the weighted sound reduction index R_w was 5–8 dB lower than that of a properly designed double panel with the same mass. But if one of the adjacent layers is left without glue, a high SRI is obtained. The transmission of the shear forces will be cancelled when the sandwich-type coupling is controlled. Sandwich-type doors are very common because of the simple manufacturing process but it is assumed that they are not appropriate as sound insulating doors without increasing the mass remarkably.

5. Two different models were used for calculating the sound transmission through apertures (sound slits). Jones' model assumed the transmission coefficient to be unity through the apertures. Gomperts' model was used for regular-shaped free apertures. The shape of the SRI-curve according to Gomperts' theory was in conformance with measurements when the slits were not sealed. The calculated slit resonance conformed with the measured position of the dip in SRI-curve. Jones' model did not give good results when the slits were free of seals. When the slits were sealed also Jones' model was found useful.

6. Sound leaks seemed to have the strongest effect on the total SRI of a door at high frequencies because of two reasons. Firstly, at low frequencies the transmission through the structure itself is usually strong and the effect of sound leaks remains quite small. Instead, at high frequencies transmission through the structure is low and even the smallest sound leaks can decrease the total SRI by several decibels. Secondly, after Gomperts' theory and after the measurements made, the SRI of a slit is about 0–10 dB at low frequencies, while at high frequencies the SRI varies in the range -15 to $+5$ dB within the slit resonance region.

7. The selection of a proper rubber seal and the smooth fitting of the door against the frames (regular clearances) are very significant factors to the total sound insulation of a door. The seal has to be flexible but still thick enough to eliminate the sound transmission through the seal itself. Additional profiles in the door edges could improve the sound insulation significantly if no rubber seals are used. If the rubber seals were properly designed and installed, the profiles were less effective.

8. The prediction models presented in this study serve as good basis for controlling and understanding the total SRI of building elements like doors, windows, walls, etc. More research is needed to find simple algebraic models to cover most typical building constructions like sandwich panels and other thin double structures. The accuracy of the prediction models for structural SRI should be improved at high frequencies.

ACKNOWLEDGMENTS

Rauno Pääkkönen is greatly appreciated for useful technical and editorial comments during writing. The financial support from the Technology Development Centre of Finland (TEKES) is appreciated.

REFERENCES

1. V. Hongisto 2000 *Journal of Sound and Vibration* **230**, 133–148. Sound insulation of doors—Part 1: prediction models for structural and leak transmission.
2. ISO/DIS 15186: 1998 Acoustics—Measurement of sound insulation in buildings and of building elements using sound intensity, Part 1: laboratory conditions. International Organization for Standardization, Genève, Switzerland.
3. V. Hongisto, K. Nieminen, H. Koskela, V. Viljanen and M. Lindgren 1997 *Noise Control Engineering Journal* **45**, 85–94. Test procedure and automatic system for sound insulation measurement using the sound intensity method.
4. Burgess 1985 *Journal of Sound and Vibration* **103**, 323–332. Resonat or effects in window frames.